

Supplemental Methods

Procedures for immunocytochemistry.

Tissue samples were collected, fixed with 0.1M phosphate-buffered formaldehyde (4%; pH 7.4; from paraformaldehyde) for 1.5 h, and washed in phosphate-buffered saline (PBS). Normal horse serum (10% for 30 min at room temp) was used to block preparations, which were then exposed to primary antibodies (CGRP, TH, Hu, GABA; 4°C; 48 - 72 hr) that were all utilized in a prior publication{Li, 2011 #1}. Bound primary antibodies were visualized with appropriate species-specific secondary antibodies labeled with contrasting fluorophores (Alexa Fluor™ 350, 488, or 594; diluted 1:200;). Preparations were washed (PBS), mounted in alkaline glycerol (66%; pH 8), and examined with a Leica CTR 6000 microscope.

Motility Studies

Colonic propulsion. Mice (10/group) were anesthetized with isoflurane (Baxter Pharmaceutical Products) and a glass bead (3 mm in diameter) was pushed with a fire-polished glass rod through the anus into the colon to a distance of 2 cm from the anal verge (Li et al., 2006). The time required for the mice to expel the bead was determined and used to estimate in vivo colorectal propulsion.

Total gastrointestinal transit time. Carmine red (300 µl; 6%; Sigma-Aldrich) suspended in 0.5% methylcellulose, which cannot be absorbed, was administered by gavage to study total GI transit time (Kimball et al., 2005). Total

GI transit time was considered as the interval between gavage and the appearance of carmine red in stool.

Gastric emptying and small intestine transit. Animals were fasted overnight in cages that lacked bedding. Water was withdrawn 3 hours before the experiment. A solution containing rhodamine B dextran (100 μ l; 10 mg/ml in 2% methylcellulose; Invitrogen) was administered to each mouse by gavage through a 21-gauge round-tip feeding needle. Animals were killed 15 min after gavage; the stomach, small intestine, cecum, and colon were collected in 0.9% NaCl. The small intestine was divided into 10 segments of equal length, and the colon (used to obtain total recovered rhodamine B fluorescence) was divided in half. Each piece of tissue was then transferred into a 14 ml tube containing 4 ml of 0.9% NaCl, homogenized, and centrifuged (2000 \times g) to obtain a clear supernatant. Rhodamine fluorescence was measured in 1 ml aliquots of the supernatant (VersaFluor Fluorometer; Bio-Rad Laboratories). The proportion of the rhodamine B dextran that emptied from the stomach was calculated as [(total recovered fluorescence - fluorescence remaining in the stomach)/(total recovered fluorescence)] \times 100. Small intestinal transit was estimated by the position of the geometric center of the rhodamine B dextran in the small bowel (Miller et al., 1981). For each segment of the small intestine (1–10), the geometric center (*a*) was calculated as follows: $a = (\text{fluorescence in each segment} \times \text{number of the segment}) / (\text{total fluorescence recovered in the small intestine})$. The total geometric center is Σ (*a* of each segment). Total geometric center values are distributed between 1 (minimal motility) and 10 (maximal

motility).

Colonic migrating motor complexes (CMMC) patterns measured in vitro.

The entire colon (5–6 cm; 5 mice/group) was removed and mounted to allow spontaneous motor patterns to be video-imaged for the construction of spatiotemporal maps (Roberts et al., 2008; Roberts et al., 2007). The isolated colon was incubated in Krebs' solution until endogenous fecal pellets were expelled. The empty colon was cannulated at both ends, mounted in a horizontal organ bath, and both luminal and serosal compartments were superfused with oxygenated Krebs' solution at 35°C. The height of a reservoir connected to the oral cannula was adjusted to maintain intraluminal pressure at +2 cm H₂O. The anal cannula provided a maximum of 2 cm H₂O back-pressure. The contractile activity was imaged with a Logitech Quickcam pro camera positioned 7–8 cm above the gut. Preparations were equilibrated for 30 min and four 15 min videos were captured. Spatiotemporal maps of the diameter at each point along the proximo-distal length of colon were constructed (Gwynne et al., 2004; Welch et al., 2014) and used to quantify the frequency of CMMCs as well as the velocity and length of their propagation. CMMCs were defined as constrictions of the diameter of the bowel that propagated for at least 50% of the length of the preparations.

Quantitation of transcripts

RNA was extracted from tissue with Trizol (Invitrogen, Carlsbad, CA) and treated with deoxyribonuclease I (1 U/mL). Polymerase chain reaction (PCR),

utilizing primers for β -actin, confirmed absence of DNA contamination. Reverse transcriptase (High Capacity cDNA Archive Kit; Applied Biosystems, Foster City, CA) was used to convert 1 μ g of sample to complementary DNA (cDNA). RT-PCR was used to quantify messenger RNA encoding interleukin 1 beta (IL1 β) or IL6. Expression of each was normalized to that of glyceraldehyde-3-phosphate dehydrogenase (GAPDH). Primers were purchased from Applied Biosystems. The real-time reaction contained cDNA (5.0 μ l), primers for the cytokine/chemokine/standard (250 nmol), PCR Master Mix (12.5 ml; Applied Biosystems), and nuclease-free water (6.25 ml). A GeneAmp 7500 sequence detection system (Applied Biosystems) was used to quantify cDNA levels. Duplicates were incubated for 2 minutes at 50°C, denatured for 10 minutes at 95°C, and subjected to 40 cycles of annealing at 60°C for 20 seconds, extension at 60°C for 1 minute, and denaturation at 95°C for 15 seconds. TaqMan 7500 software (Applied Biosystems, Foster City, CA) was used for data analysis.

Parameters of mucosal maintenance

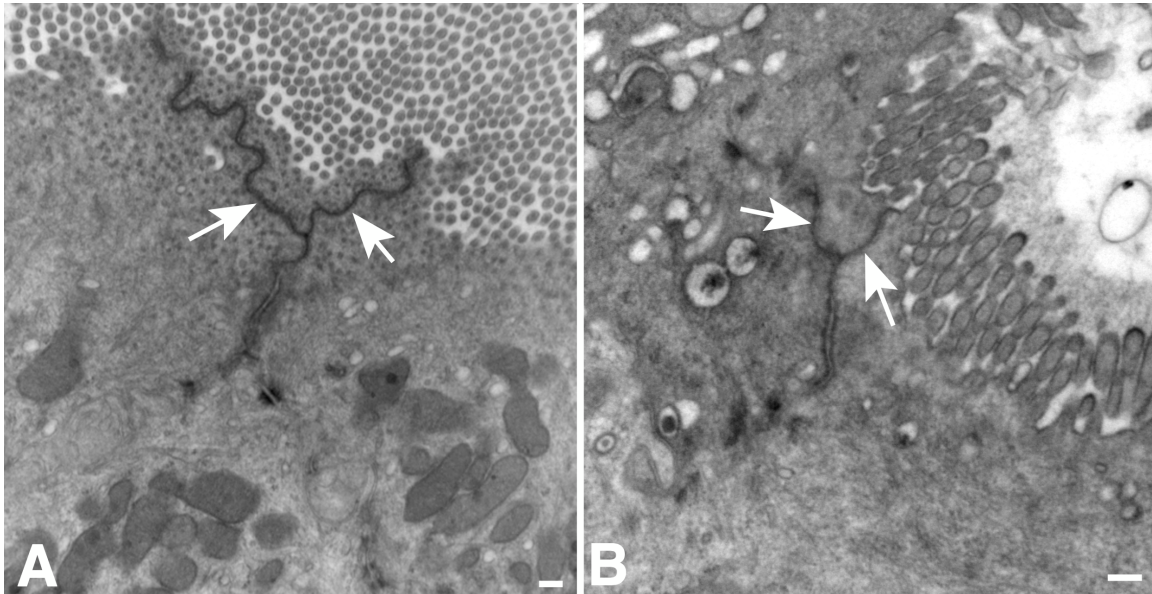
Segments of colon and small intestine were fixed, for 3 hours at room temperature as described above. Fixed tissue was embedded in paraffin, sectioned at 10 μ m, and stained with hematoxylin and eosin. Computer-assisted imaging (VLOCITY 6.0 software) was employed to measure villus height and crypt depth (Gross et al., 2012). Villi (≥ 20 /mouse) were measured when the central lacteal was completely visualized. Crypts (≥ 20 /mouse) were analyzed when the crypt–villus junction could be visualized on both sides of the crypt.

Sympathetic denervation.

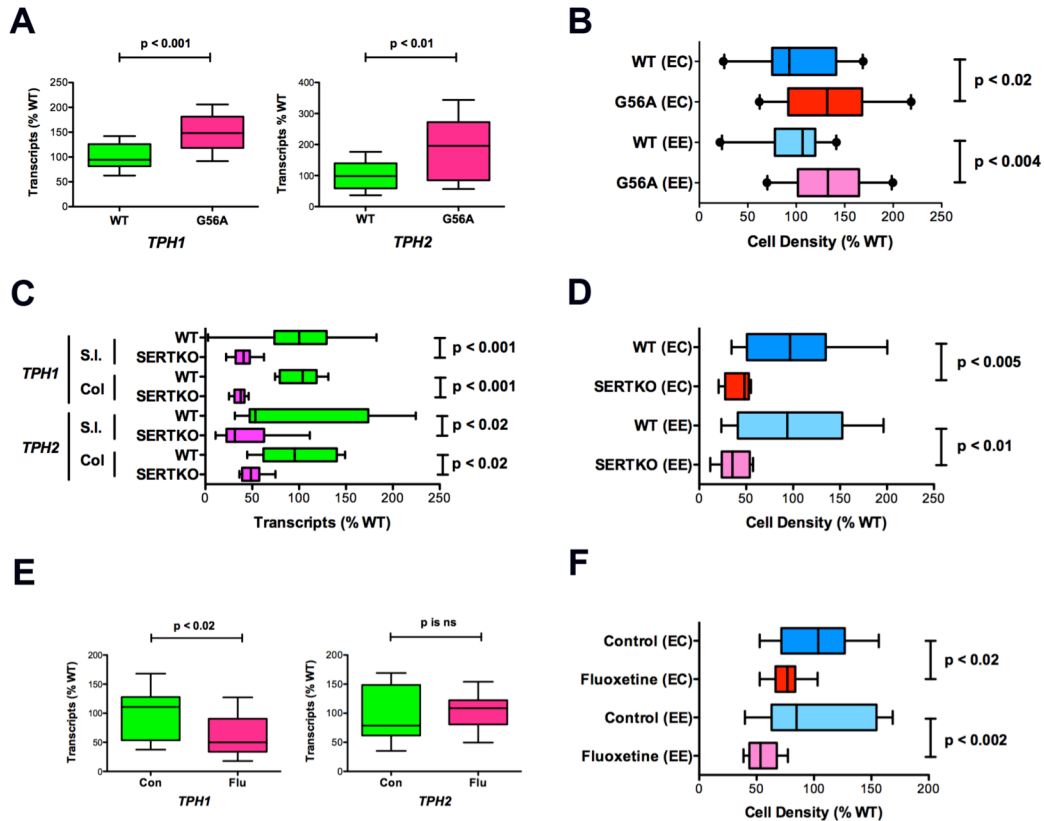
Intraperitoneal administration of 6-hydroxydopamine (6-OHDA; 100 mg/kg; Sigma-Aldrich) in 0.5 % ascorbic acid was used to chemically sympathectomize mice. This treatment induces the destruction of almost all intestinal sympathetic nerve fibers within 3–5 days (Gershon and Sherman, 1982; Gershon et al., 1980).

Electron microscopic evaluation of tight junctional integrity.

Horseradish peroxidase (HRP; Sigma type VI; 1 mg/gram body weight) dissolved in 0.1 ml PBS was injected into the tail veins of mice. Animals were euthanized 5 minutes later and segments of small intestine and colon were removed (n=3 mice/group). Tissues were fixed with 2.5% glutaraldehyde. Small tissue blocks were cut and incubated with 3, 3'-diaminobenzidine (DAB) and H₂O₂, generated from a glucose/glucose oxidase generating system to locate sites of peroxidase activity (Gershon et al., 1994). The tissue blocks were dehydrated and embedded for sectioning. Sections were cut at 0.6 nm and either counterstained with uranyl acetate and lead citrate or left unstained to visualize DAB. Sections were examined with a JEOL 1200EX electron microscope.

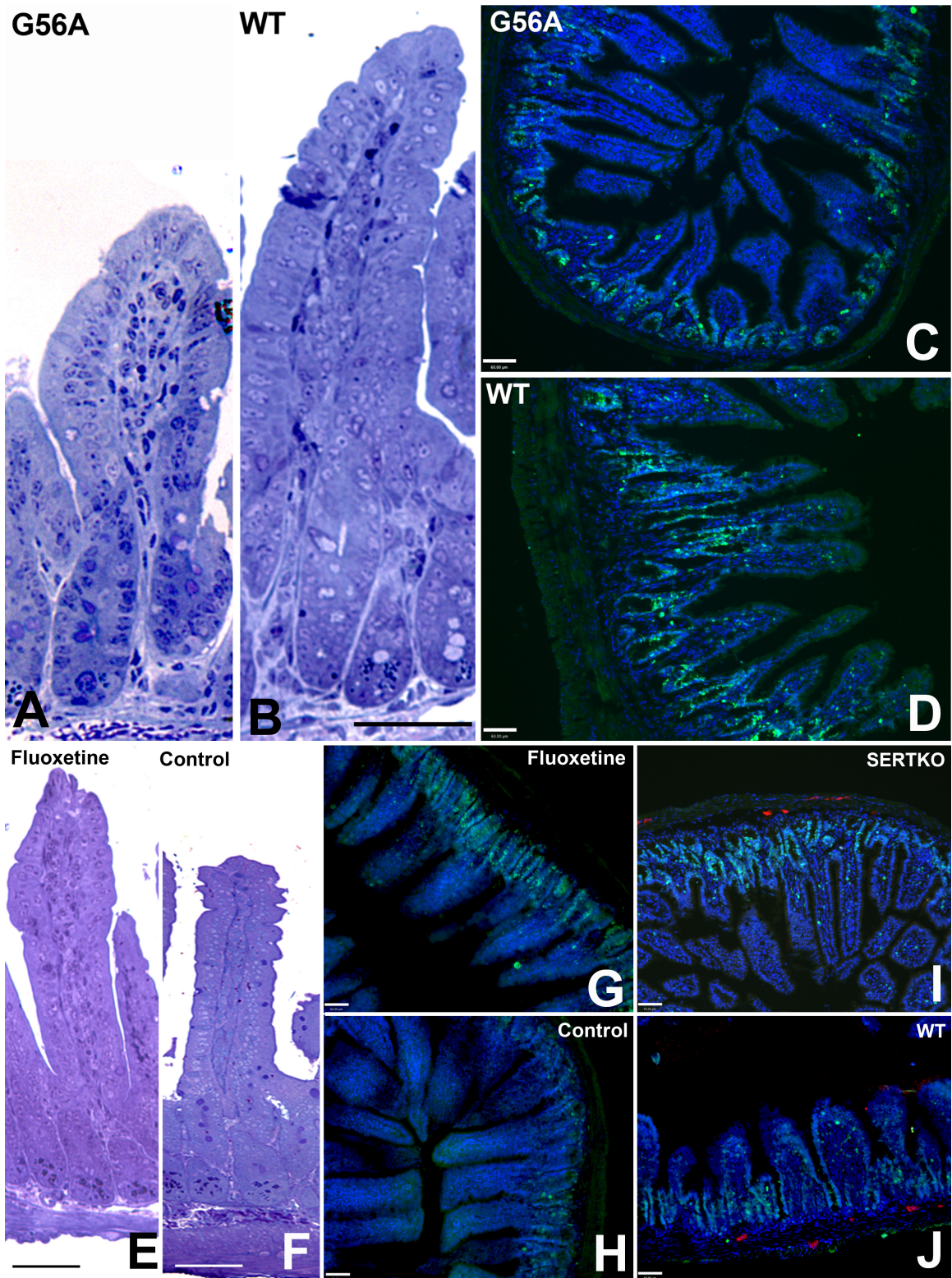


Supplemental Fig. 1. Tight junctions between enterocytes block the transepithelial passage of HRP from the extracellular space to the small intestinal lumen. WT and SERT Ala56 mice were injected intravenously with HRP and the ileum was removed and fixed min later. Peroxidase activity was demonstrated histochemically with DAB and the tissue was examined electron microscopically. A. WT. B. SERT Ala56. The arrows point to the intercellular space basal to the apical tight junctions between adjoining enterocytes in which the dark reaction product of HRP can be seen to have accumulated. The markers = 250 nm.



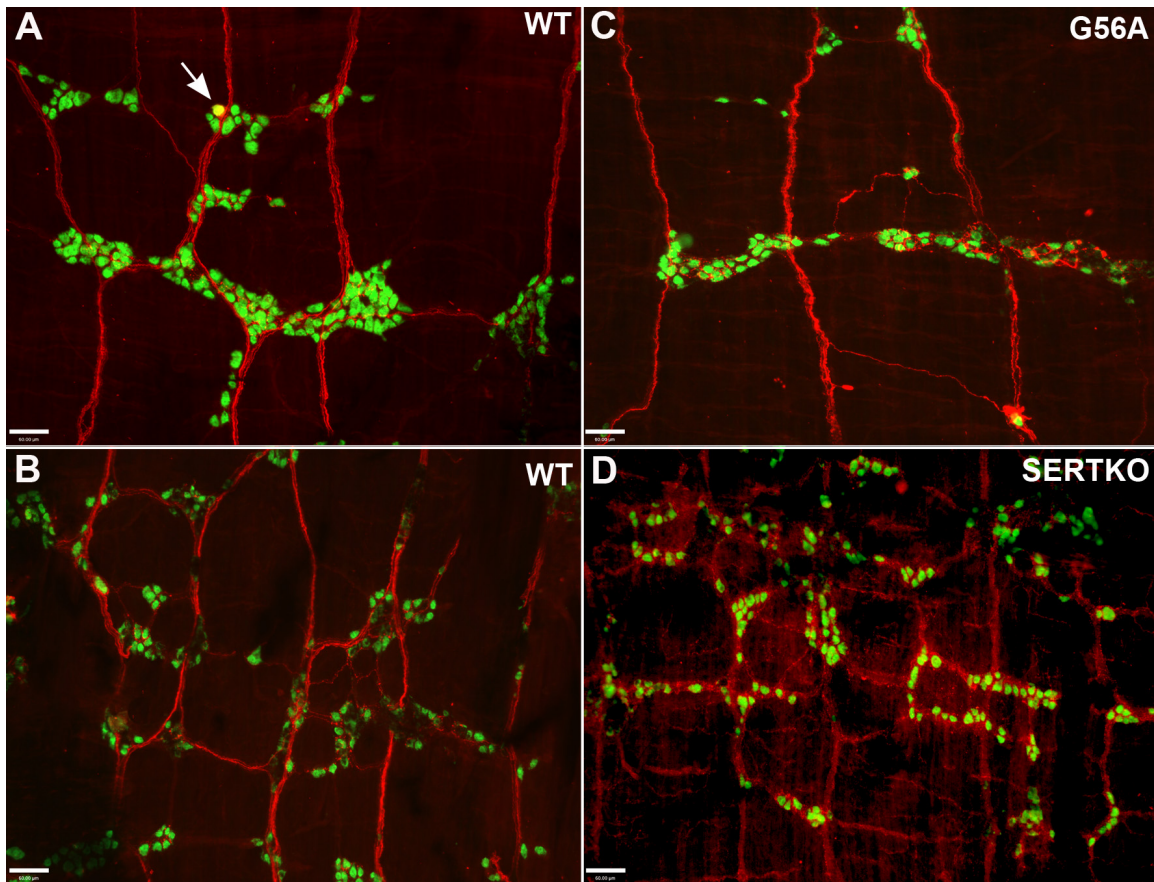
Supplemental Fig. 2. The effects of the SERT Ala56 mutation in SERT on transcription of TPH1 and TPH2 as well as on EC and total EE cell numbers are the opposite of those seen in SERTKO mice and animals treated during development with fluoxetine. A. Comparison of transcription of TPH1 and TPH2 in WT and SERT Ala56 (G56A) mice. Both TPH isoforms are more abundant in SERT Ala56 than in WT mice. B. Comparison of numbers of EC and total EE cells in WT and SERT Ala56 (G56A) mice. Both EC and total EE cells are more abundant in SERT Ala56 than in WT mice. C. Comparison of transcription of TPH1 and TPH2 in WT and SERTKO mice. Both TPH isoforms are more abundant in WT than in SERTKO (KO) mice. D. Comparison of numbers of EC and total EE cells in WT and SERTKO mice. Both EC and total EE cells are more

abundant in WT than in SERTKO mice. E. Comparison of transcription of TPH1 and TPH2 in control and mice treated during development with fluoxetine. TPH1 but not TPH2 is more abundant in WT than in fluoxetine-treated mice. F. Comparison of numbers of EC and total EE cells in control and mice treated during development with fluoxetine. Both EC and total EE cells are more abundant in WT than in fluoxetine-treated mice.



Supplemental Fig. 3. Villus height, crypt depth, and the proliferation of crypt

epithelial cells are all less than WT in SERT Ala56 (G56A) small intestine but greater than control or WT in fluoxetine-treated and SERTKO mice. The small intestine was fixed, embedded in plastic (Epon 812) and sectioned at 1 μm to view villus height and crypt depth (panels A, B, E and F). To evaluate proliferation, the small intestines were fixed, cryosectioned, and immunostained with antibodies to Ki67 (panels, C, D, G-J). A. A representative villus and associated crypts from a SERT Ala56 (G56A) mouse. B. A representative villus and associated crypts from a WT mouse. C and D. Cross-sections of small intestine from a SERT Ala56 (C) and WT mouse (D) immunostained to show Ki67 (green) and DNA (blue). The images are merged. Note that Ki67-immunoreactive cells are more abundant in the WT than in the SERT Ala56 mouse. E. A representative villus and associated crypts from a fluoxetine-treated mouse. F. A representative villus and associated crypts from a control mouse. G and H. Cross-sections of small intestine from fluoxetine-treated (G) and control mouse (H) as well as a SERTKO (I) and a WT (J) mouse immunostained to show Ki67 (green) and DNA (blue). The SERTKO (I) and WT (J) tissues were also immunostained with ANNA-1 antibodies (red) to show the locations of the enteric plexuses. The bars = 60 μm .



Supplemental Fig. 4. 5-HT-immunoreactive neurons are hypoplastic in SERT Ala56 (G56A) mice and hyperplastic in SERTKO animals. Longitudinal muscle and attached myenteric plexus were mechanically dissected from WT, SERT Ala56 (G56A), and SERTKO mice. Neurons and 5-HT were immunostained, respectively with ANNA-1 antibodies (green) and antibodies to 5-HT (red). The proportion of neurons that is serotonergic is low but the long axons of serotonergic neurons are abundant. A. WT mouse (a serotonergic neuron (arrow) appears yellow because it is co-immunostained with ANNA-1 and 5-HT antibodies. B. (compare with A) SERT Ala56 (G56A). C. WT. D. SERTKO. (compare with C) Note that the intensity of 5-HT immunofluorescence is lower in

SERTKO than in WT gut because of the impaired re-uptake of 5-HT. Note also that the pattern of 5-HT-immunoreactive fibers is different. Branching in ganglia is more extensive than in WT gut and fibers are more coarse.